Journal of Applied Electrochemistry **30**: 987–994, 2000.

Effect of tartrate on the morphological characteristics of the copper–tin electrodeposits from a noncyanide acid bath

I.A. CARLOS[1]*, C.A.C. SOUZA[1], E.M.J.A. PALLONE[2], R.H.P. FRANCISCO[3], V. CARDOSO[3] and B.S. LIMA-NETO[3]
[1]*Departamento de Química, Universidade Federal de São Carlos, CP 676, 13565-905, São Carlos-SP, Brazil*
[2]*Departamento de Engenharia de Materiais, UFSCar, São Carlos-SP, Brazil*
[3]*Instituto de Química de São Carlos, USP, São Carlos-SP, Brazil*
*(*author for correspondence, e-mail: ivani@dq.ufscar.br)*

Received 12 August 1999; accepted in revised form 29 February 2000

Key words: copper–tin alloys, noncyanide bath, platinum electroplating, tartrate as additive

Abstract

Copper and tin were electrodeposited on platinum substrates from a 1.0 M sulphuric acid plating bath in the presence and absence of tartrate. Voltammetric curves indicated two deposition processes, at −0.310 and −0.640 V, which do not shift upon addition of tartrate to the plating bath. The presence of tartrate decreased the current density in the region of the more cathodic process. The metals were electrodeposited at both deposition potentials and the deposits have the same proportions of copper and tin either with or without tartrate in the plating bath, as observed by AAS. X-ray spectra suggested that a mixture of Cu and η-Cu_6Sn_5 alloy was deposited at the less cathodic potential. SEM analysis showed that tartrate affects the morphology of the films.

1. Introduction

In view of attractive features, such as resistance to corrosion, malleability, ductility and solderability, Cu–Sn alloys have been widely used in industry [1–6]. Commercial electrodeposition of Cu–Sn alloys based on cyanide baths produces high quality deposits [1, 7] but causes environmental problems in the use and disposal of cyanide. To develop an alternative Cu–Sn plating bath that avoids the use of cyanide, we have studied a sulphuric acid bath using tartrate as additive. This choice of bath resides in the fact that the presence of the organic additive potassium sodium tartrate has led to acceptable silver deposits, as the additive acts as an effective growth inhibitor in acid plating [8–10]. The acid medium is required as tartrate decomposes during electrolysis from an alkaline Cu–Sn plating bath [1]. Accordingly, the electrodeposition studies described here are designed to evaluate the effect of potassium sodium tartrate on the characteristics of Cu–Sn deposits from an acid bath.

2. Experimental details

All chemicals are analytical grade. Double distilled water was used throughout. Each electrochemical experiment was performed in a freshly prepared noncyanide bath, containing 0.12 M $CuSO_4$ and/or 0.10 M $SnCl_2$, and 1.0 M H_2SO_4, either in the absence or presence of 0.25 M potassium sodium tartrate. A Pt disc (0.396 cm^2), a Pt plate and a normal calomel electrode (NCE) with an appropriate Luggin capillary, were employed as working, auxiliary and reference electrodes, respectively. When indicated, the Pt was replaced by Cu (0.302 cm^2) or Sn (0.363 cm^2) disc electrodes. Immediately prior to the electrochemical measurements, the Pt working electrode was dipped in a sulphuric–nitric acid solution, while the Cu and Sn disc electrodes were ground with 600 emery paper; then, after being rinsed with water these electrodes were dipped in an ultrasonic bath for about 1 min, and rinsed again. Potentiodynamic curves were recorded using a PARC electrochemical system consisting of a model 173 potentiostat/galvanostat, at a scanning rate of 10 mV s^{-1}. All experiments were carried out at room temperature (25 °C). Potentiostatic deposits were obtained at 2.56 C cm^{-2}. The deposition current efficiencies (ϕ_e), in the absence and presence of tartrate, were obtained from the stripping/deposition charge ratio [11, 12].

The Cu and Sn contents of the deposits were analysed by atomic absorption using an Interlab atomic absorption spectrophotometer (AAS), model AA12/1475, after anodic stripping in a 1.0 M H_2SO_4 solution.

X-ray diffraction patterns were produced with filtered Cu$K\alpha$ radiation (154.051 pm), using a Carl Zeiss URD6 automatic diffractometer set at 40 kV and 20 mA,

running in the $\omega/2\theta$ scanning mode. Trials with fixed ω did not improve the results.

Scanning electron microscopy (SEM) photographs were taken with a Carl Zeiss (model DSM 940A) electron microscope with 4 nm resolution.

Energy dispersive X-ray spectroscopy (EDS) readings were taken with a Zeiss/Leica (model LEO 440), EDS Si/Li, Be ultrathin window.

3. Results and discussion

3.1. *Electrodeposition of Cu–Sn in the absence of tartrate*

Figure 1 shows a typical voltammogram for the stationary platinum electrode in the Cu–Sn plating bath. The main features of this voltammogram are two cathodic peaks (a, b) and the anodic processes a′, b′, b″ and b‴. The increase in the current density at potentials more negative than −0.9 V can be related to hydrogen evolution.

Bearing in mind that the electrode surface composition undergoes a continuous change during the cathodic deposition, Pt, Cu and Sn electrodes were studied to obtain the hydrogen evolution overpotentials in the absence of the plating salts. The cathodic voltammograms for these substrates do not show any current up to approximately −1.2, −0.8 and −0.4 V, respectively (insert Fig. 1), suggesting that hydrogen evolution is not a significant side reaction during the initial stages of the plating process. Indeed, it is only important beyond the region of peak b.

The reactions occurring in each cathodic process were identified by recording voltammetric curves for each metal ion under the same conditions (Figures 2 and 3). Figure 2 shows voltammograms recorded for the Pt substrate using only the Cu salt (broken line) or both Cu and Sn salts (solid line) in the plating solutions. As can be seen, the Cu deposition (broken line) begins around −0.2 V. Comparing this curve with the Cu–Sn potentiodynamic curve (solid line), peak a can be associated with Cu plating or Cu–Sn alloys or both. This result agrees with those observed for Cu–Sn alloy eletrodeposited from a pyrophosphate bath and also with the finding that the reversible potential of the alloy is in the same region as the reversible potential of copper [13], as observed in the present case (Figure 2). Figure 3 presents two voltammograms recorded for the Pt substrate using only the Sn salt (broken line) or both Cu and Sn salts (solid line), in the plating solutions. In the case of the Sn salt plating solution (broken line), there is no current down to about −0.6 V in the forward scan, then the cathodic current increases steeply.

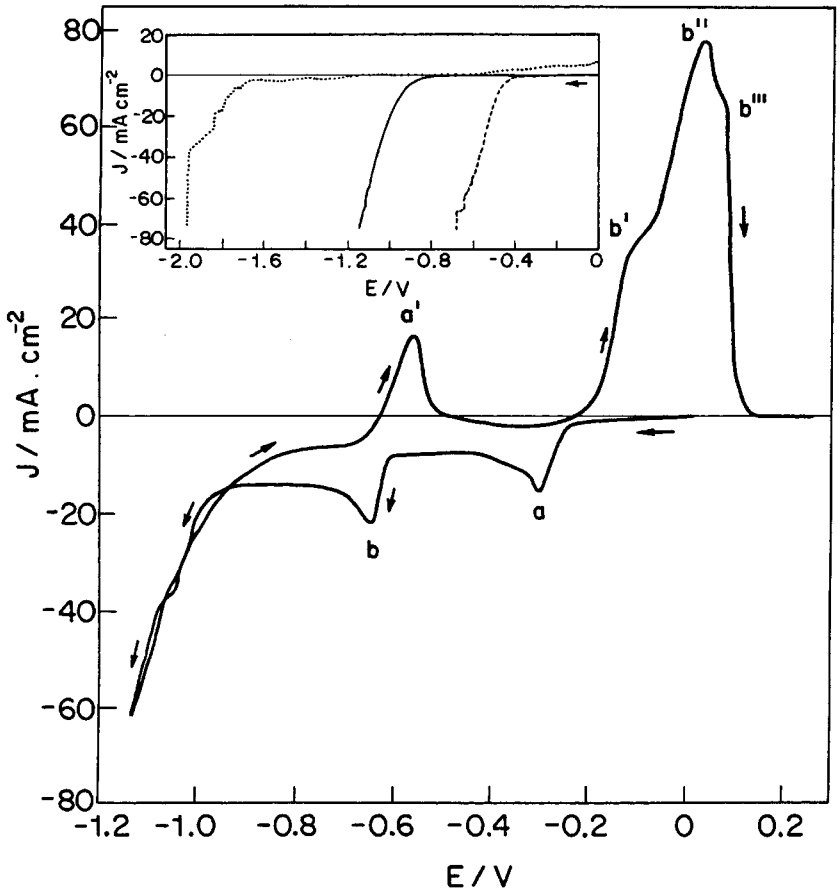

Fig. 1. Voltammetric curve for Pt substrate in 0.12 M $CuSO_4$, 0.10 M $SnCl_2$ and 1.0 M H_2SO_4, at 10 mV s^{-1}. Insert: Voltammetric curves for Pt (broken line), Cu (solid line) and Sn (dotted line) substrates in 1.0 M H_2SO_4, at 10 mV s^{-1}.

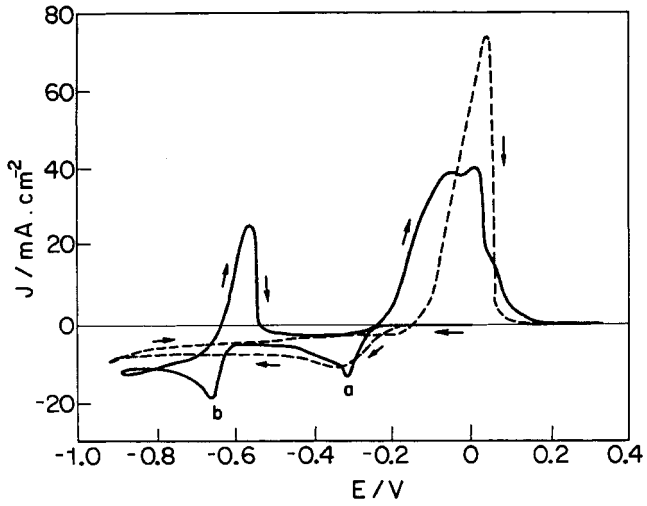

Fig. 2. Voltammetric curves for Pt substrates in 0.12 M $CuSO_4$, 0.10 M $SnCl_2$ and 1.0 M H_2SO_4 (solid line), and in 0.12 M $CuSO_4$ and 1.0 M H_2SO_4 (broken line), at 10 mV s^{-1}. Characters a and b correspond to the cathodic peaks in the solid line.

Comparing this voltammogram (solid line) with the Cu–Sn potentiodynamic curve (solid line), peak b can be associated with Cu–Sn alloys or a mixture of Sn and Cu–Sn alloy plating.

To characterise the cathodic process better in the region of peak a, the sweep was reversed at several potentials (Figure 4): at potentials less cathodic than −0.34 V (solid line), at −0.34 V (dotted line), and at potentials more negative than −0.34 V (broken line). Analysing the dissolution process, anodic peaks and

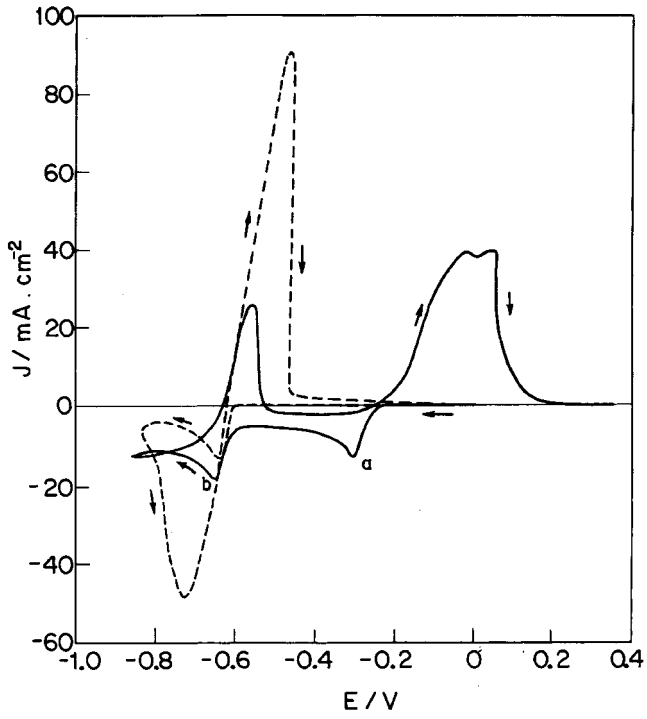

Fig. 3. Voltammetric curve for Pt substrates in 0.12 M $CuSO_4$, 0.10 M $SnCl_2$ and 1.0 M H_2SO_4 (solid line), and in 0.10 M $SnCl_2$ and 1.0 M H_2SO_4 (broken line), at 10 mV s^{-1}. Characters a and b correspond to the cathodic peaks in the solid line.

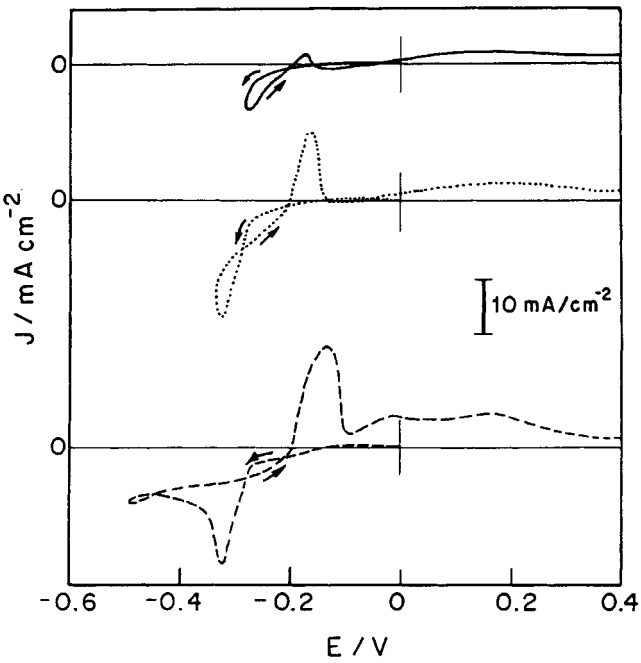

Fig. 4. Voltammetric curves for Pt substrates in 0.12 M $CuSO_4$, 0.10 M $SnCl_2$ and 1.0 M H_2SO_4 in absence of potassium sodium tartrate effect of the cathodic potential limit values (10 mV s^{-1}): solid line: at potential less cathodic than −0.34 V, dotted line: at −0.34 V and broken line: at potential more negative than −0.34 V.

humps were observed, which increase as the amount of the deposited metal increases, since the cathodic sweep was reversed at potentials more and more negative. These anodic processes can be correlated with the processes b′, b″ and b‴ in Figure 1. The presence of several anodic processes suggests that tin deposition commences in the region of peak a and alloys are probably formed. If tin were not deposited in the region of peak a, only the anodic peak corresponding to dissolution of pure copper would be observed, as in Figure 2 (dotted line). Thus, from these studies, a codeposition of copper and tin can be characterised already in the region of peak a. Furthermore, in the voltammograms of Figure 4, distinct processes can be seen at different reversal potentials. At potentials less cathodic than −0.34 V (solid line), an increase in cathodic current and a nucleation loop are observed, which suggests that the metal deposition occurred by nucleation [14]. When the sweep was reversed at −0.34 V (dotted line), the current decreased, indicating that the plating process was under diffusion control [15]. Finally, when the sweep was reversed at potentials more negative than −0.34 V (broken line), the current increased and also a nucleation loop is observed, suggesting another nucleation process, as in the first case (solid line).

3.2. *Electrodeposition of Cu–Sn in the presence of tartrate*

Figure 5 illustrates voltammetric curves for the Pt electrode in the Cu–Sn plating bath, in the presence and absence of tartrate, showing cathodic and anodic

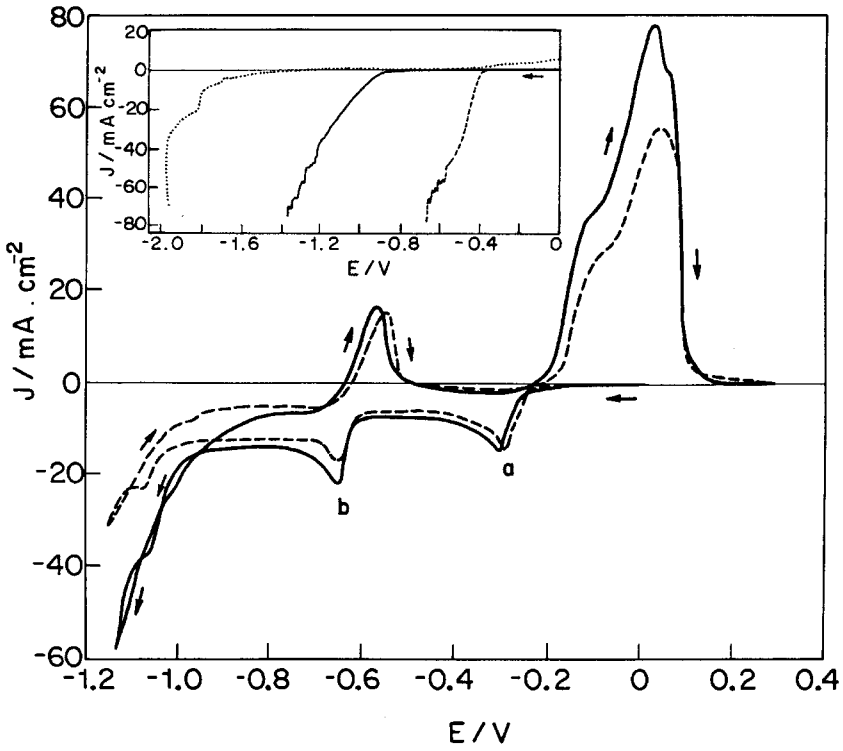

Fig. 5. Voltammetric curves for Pt substrates in 0.12 M $CuSO_4$, 0.10 M $SnCl_2$ and 1.0 M H_2SO_4, in absence (solid line) and presence (broken line) of 0.25 M potassium sodium tartrate, at 10 mV s^{-1}. Insert: Voltammetric curves for Pt (broken line), Cu (solid line) and Sn (dotted line) substrates in 1.0 M H_2SO_4 and 0.25 M potassium sodium tartrate, at 10 mV s^{-1}.

processes. The presence of tartrate does not shift the deposition potentials, but reduces the deposition current density in the region of peak b. The fact that the presence of tartrate does not shift the deposition potentials suggests that it does not form complexes with Cu^{2+} or Sn^{2+} ions to a significant extent. This might be expected since the tartrate must be protonated at the high acidity of the medium (final pH 0.25). The tartrate acid pK_a values are 3.8 and 2.8 [16].

To understand the reduction of the deposition current density in the region of peak b in the presence of tartrate (Figure 5), voltammetric recordings were carried out in two different baths, each containing only one of the metal ion species (Figures 6 and 7). As can be seen in these Figures, tartrate reduces only the Sn deposition current density (Figure 7). The ϕ_e values, in the presence and absence of tartrate, Figure 7, are seen to be roughly the same (87 and 90%, respectively). These results can be interpreted as an inhibition of the deposition process in the region of peak b, or a modification in the morphology of the Sn deposit. Such a morphological change was also observed during silver electrodeposition from a nitrate plating bath, where inhibition of dendrite growth took place [8–10]. This may explain the difference in the current density values for the Cu–Sn deposit in the region of peak b (Fig. 5). The ϕ_e values obtained during the potentiodynamic deposition up to the final potential (−0.820 V), in the presence and absence of tartrate, are 64 and 61%, respectively; also modification in the morphology of the deposit was observed by SEM and this will be discussed later.

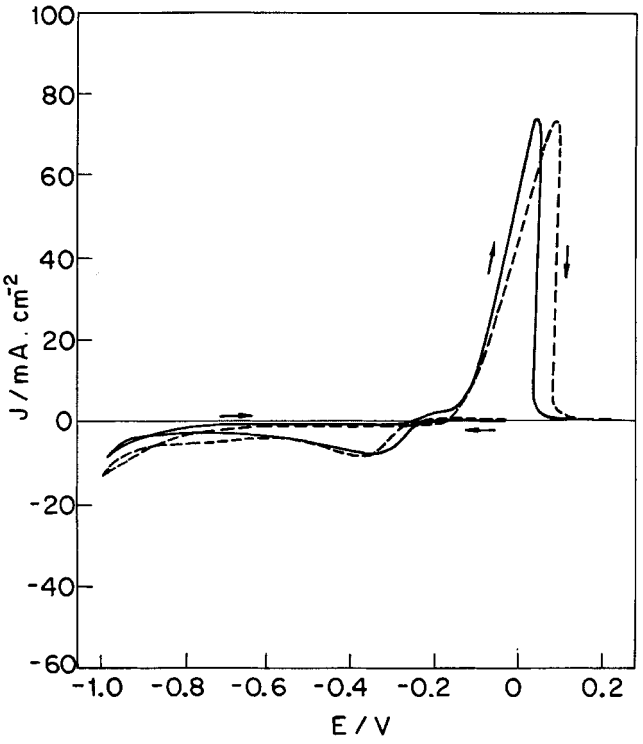

Fig. 6. Voltammetric curves for Pt substrates in 0.12 M $CuSO_4$ and 1.0 M H_2SO_4, in absence (solid line) and presence (broken line) of 0.25 M potassium sodium tartrate, at 10 mV s^{-1}.

These results are very significant since the presence of tartrate in the plating bath could lead to a better quality deposit.

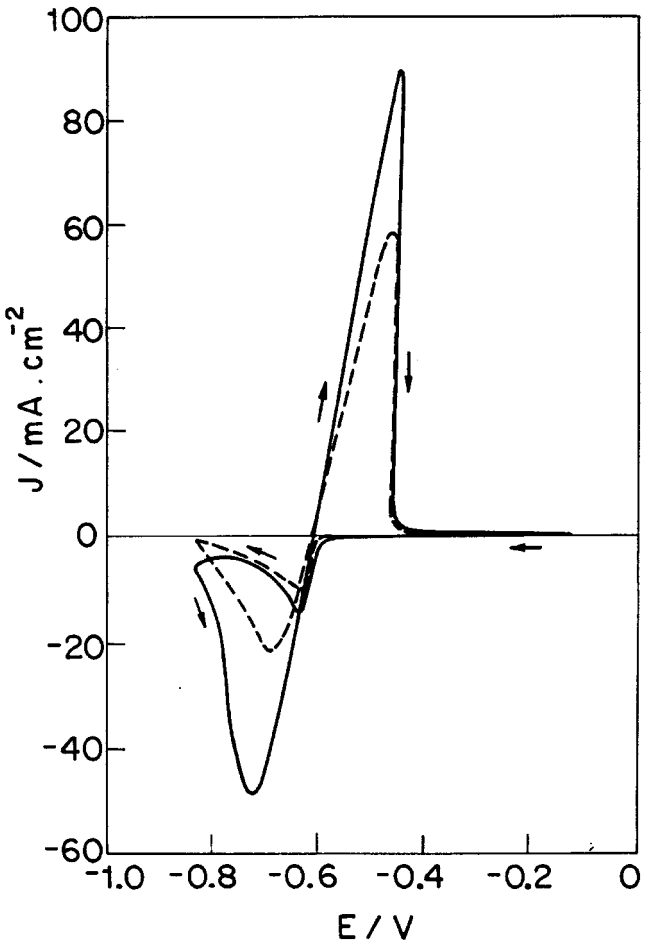

Fig. 7. Voltammetric curves for Pt substrates in 0.10 M $SnCl_2$ and 1.0 M H_2SO_4, in absence (solid line) and presence (broken line) of 0.25 M potassium sodium tartrate, at 10 mV s^{-1}.

The hydrogen evolution overpotentials for the different Cu, Sn and Pt electrodes in the presence of tartrate are the same as in its absence (inserts Figures 1 and 5). Thus, as already observed in Figure 1, hydrogen evolution does not affect the Cu–Sn voltammetric deposition in the initial stages of the process. It is only really significant at potentials beyond −0.8 V.

Reversing the sweep at various cathodic potentials, with tartrate present in the plating bath, produced results similar to those without tartrate (Figure 4).

3.3. *AAS analysis of the Cu–Sn deposits in the absence and presence of tartrate*

To verify the nature of the deposit at peaks a and b (Figure 5), analyses by atomic absorption spectrophotometry (AAS) were carried out after anodic stripping. The results showed that deposition of both Cu and Sn occurs at both peaks, either in the absence or presence of tartrate (Table 1). Roughly the same percentage of Cu or Sn metal are obtained at peak a, whether in the absence or in the presence of tartrate in the plating bath. This is also observed at peak b. In addition, each metal is electrodeposited in a greater amount at its own cathodic potential (Cu at peak a, Sn at peak b). This means that, when the potential is changed from −0.310 V (peak a) to −0.640 V (peak b), the Cu content decreases from approximately 68% to about 46%, and the Sn content increases from 32% to about 54%, in the absence of tartrate. Similar behaviour is observed in the presence of tartrate. Thus, the Cu–Sn ratio is higher at the first cathodic process (peak a) than at the second one (peak b), either in absence or presence of the additive. This agrees with the colour of the resulting deposits, where in the former process a reddish colour was observed while in the latter, a grayish colour was noted.

Table 1. Contents* of Cu and Sn electrodeposited from a plating bath† in absence and presence of tartrate, at each cathodic peak‡, with Q = 2.56 C cm^{-2}

Peaks	Mass of Cu, mg (%)	Mass of Sn, mg (%)
Peak a, absence of tartrate	0.188 (68.2)	0.088 (31.8)
Peak b, absence of tartrate	0.084 (45.6)	0.100 (54.4)
Peak a, presence of tartrate	0.186 (66.2)	0.095 (33.8)
Peak b, presence of tartrate	0.094 (50.5)	0.093 (49.5)

*Average value of three independent experiments
†[$CuSO_4$] = 0.12 M, [$SnCl_2$] = 0.10 M and [H_2SO_4] = 1.0 M
‡Peak a = −0.310 V; peak b = −0.640 V

The fact that in the presence of Cu, Sn begins to electrodeposit at a more positive potential than in the bath containing only Sn, suggests that Cu has a synergetic effect on deposition of Sn. Since copper is a nobler metal than tin, the deposition process can be initiated by discharge (nucleation) of the nobler component (copper), after which Cu–Sn interactions make possible the deposition of the less noble component (tin) [17]. Krogër [17] has suggested that this is possible when the concentration of the nobler component (copper) is lower than the less noble component (tin). However, in the present case the copper and tin concentrations in the plating bath are basically the same, and experiments described by Despić [13] have shown Cu–Sn deposition, where the copper concentration is higher than that of the tin. On the other hand, Tu ascertained that Cu reacts with Sn at room temperature to form the compound Cu_6Sn_5 [5,18]. Furthermore, the possibility of interaction between copper and tin in the solid phase is indicated by the Cu–Sn phase diagram [19].

Finally, it can be concluded from the potentiodynamic curves for the Pt electrode in the Cu, Sn and Cu–Sn plating baths, and also from the AAS analysis of the solutions obtained by stripping the Cu–Sn deposits, that peak a can be associated with a deposit of Cu and Sn, richer in Cu, and peak b with a Cu and Sn deposit with the same amount of each metal.

3.4. *X-ray analysis of the Cu–Sn deposits in the absence and presence of tartrate*

Figure 8 shows X-ray diffraction patterns of deposits obtained from a solution of Cu and Sn salts, at a

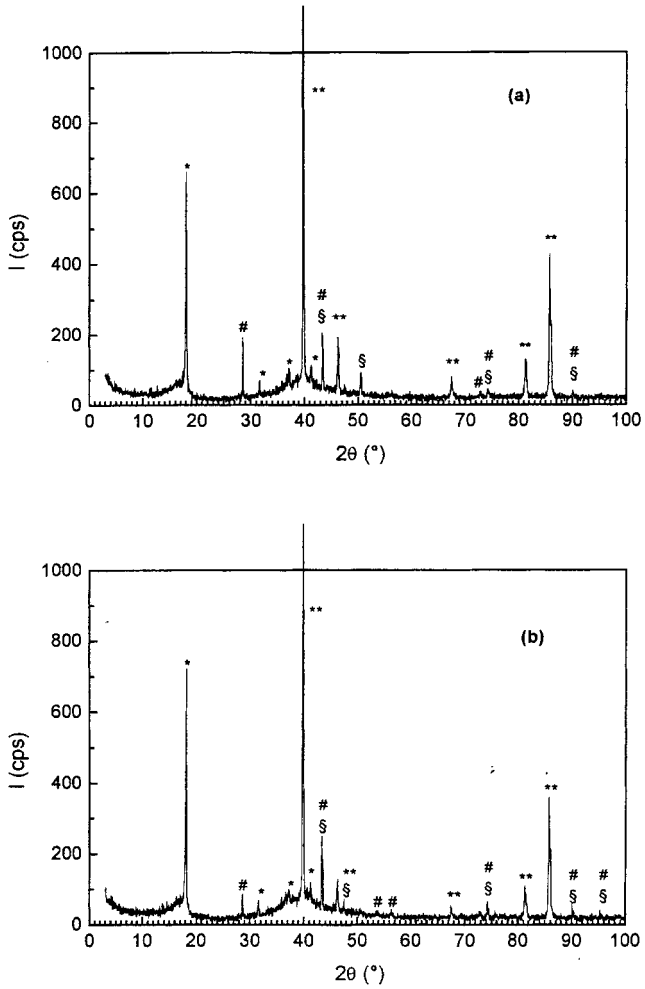

Fig. 8. Diffractograms of deposits obtained at −0.310 V and 2.56 C cm^{-2}, on Pt support. Four compounds are present: Teflon (*), Pt (**), η-Cu_6Sn_5 (#, JCPDS-2-713), Cu (§, JCPDS 4-836). (a) In the absence of tartrate; (b) in the presence of tartrate.

deposition potential of −0.310 V, which is favourable to copper deposition. The experiment was done both in the presence and in the absence of tartrate to investigate its influence on the crystalline characteristics of the deposits. The observed crystallographic distances, $d(h\,k\,\ell)$, and expected values from phases described in JCPDS [20] are in Table 2. Most of the peaks are due to the Pt substrate where the film was deposited and to the Teflon piece, used to fix the sample.

The diffraction experiment was done using $\omega/2\theta$ scan. It was repeated with 2θ scan (fixing $\omega = 3°$), without achieving a better resolution. In one experiment, the deposit was detached from the support using an adhesive tape. The diffractograms from the deposits obtained at −0.310 V, in the absence or in the presence of tartrate, showed similar patterns (Figure 8) and indicated the occurrence of η-Cu_6Sn_5 and copper (Table 2). These results are compatible with the content of Cu (∼67%) and Sn (∼33%) obtained by AAS analysis, where the total copper content comes from the dissolution of η-Cu_6Sn_5 alloy, whose composition is ∼40% Cu and ∼60% Sn [19], plus dissolution of pure copper. The Sn content comes only from the dissolution of η-Cu_6Sn_5 alloy.

Table 2. Observed interplanar distances, $d(h\,k\,\ell)$, of X-ray diffraction pattern of Cu/Sn deposits obtained at potential −0.310 V and 2.56 C cm^{-2}, in the absence ($d_1(h\,k\,\ell)$) or presence ($d_2(h\,k\,\ell)$) of tartrate

Expected values are from JCPDS [16]: η-Cu_6Sn_5 (2-713), Cu (4-836), Pt (4-802)

Expected values above 10% of relative intensity were selected

Observed values for Teflon were obtained experimentally

$d_1(h\,k\,\ell)$ obs	$d_2(h\,k\,\ell)$ obs	d_{exp} η-Cu_6Sn_5	d_{exp} Cu	d_{obs} Teflon	d_{exp} Pt
4.91	4.90			4.91	
3.130	3.122	2.96			
2.825	2.818			2.82	
		2.55			
2.422	2.422			2.41	
2.264	2.264				2.265
2.179	2.179			2.18	
2.083	2.086	2.09	2.088		
		2.08			
1.957	1.951				1.9616
1.800			1.808	1.84	
	1.702	1.71			
	1.626	1.62			
		1.54			
		1.48			
1.388	1.387				1.3873
1.301		1.32		1.30	
1.274	1.277	1.27	1.278	1.25	
		1.24			
		1.21			
		1.20			
1.184	1.182				1.1826
1.132	1.132				1.1325
1.089	1.089	1.090	1.090		
		1.070			
	1.041	1.050	1.0436		

Some diffraction lines are more easily assigned to η-Cu_6Sn_5 and/or Cu in Figure 8(b), where the electrodeposit was obtained in the presence of tartrate. However, there is no clear change in the degree of crystallinity upon the addition of tartrate. It is hard to take the discussion about the crystalline and amorphous character of Cu–Sn deposits further, since the diffractograms look the same with respect to the line width.

The deposits obtained at −0.640 V do not generate a good diffraction pattern. All the trials revealed only the Pt-support pattern. The experiment using 2θ scan (fixing $\omega = 3°$) failed to reveal any crystalline phase. Attempts to scrape the deposit from the support did not succeed, indicating its strong adhesion. Also, attempts to prepare thicker deposits to have better signals have failed, since the deposits become darker and more porous with time.

3.5. *Scanning electronic microscopy*

Figure 9 shows SEM micrographs of films formed at −0.310 V in the absence and presence of tartrate. By comparing these micrographs it can be observed that the

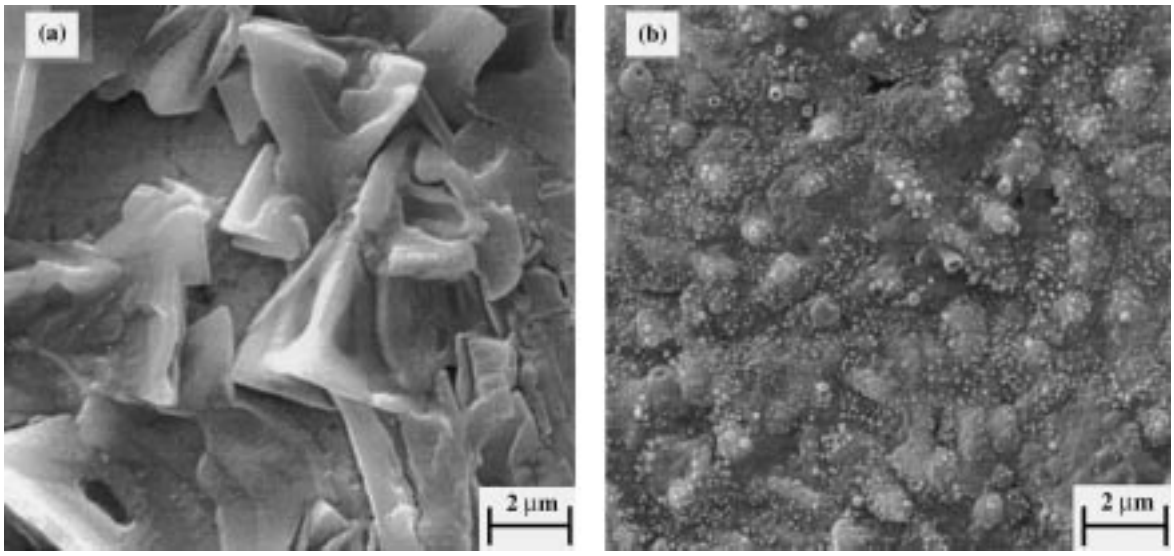

Fig. 9. SEM micrographs of Cu–Sn films obtained at $E = -0.310$ V and 2.56 C cm^{-2}. Electrolytic solutions: (a) 0.12 M $CuSO_4$, 0.10 M $SnCl_2$ and 1.0 M H_2SO_4, (b) 0.12 M $CuSO_4$, 0.10 M $SnCl_2$, 1.0 M H_2SO_4 and 0.25 M potassium sodium tartrate. Thickness of Cu–Sn films 172 μm.

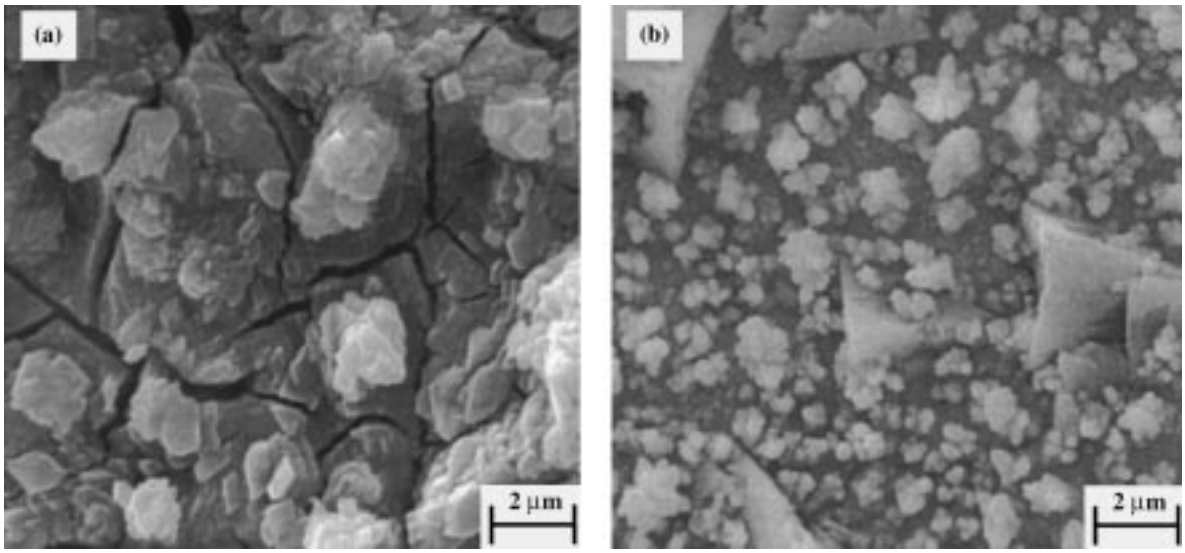

Fig. 10. SEM micrographs of Cu–Sn films obtained at $E = -0.640$ V and 2.56 C cm^{-2}. Electrolytic solutions: (a) 0.12 M $CuSO_4$, 0.10 M $SnCl_2$ and 1.0 M H_2SO_4, (b) 0.12 M $CuSO_4$, 0.10 M $SnCl_2$, 1.0 M H_2SO_4 and 0.25 M potassium sodium tartrate. Thickness of Cu–Sn films 172 μm.

morphologies of the films change when tartrate is present: the grains become more uniform.

Figure 10 shows SEM micrographs of films formed at −0.640 V in the absence and presence of tartrate. The most noticeable features are the presence of nodules and cracks in the absence of tartrate (Figure 10(a)). The cracks suggest that the deposits are stressed and they are eliminated when the electrodeposition is carried out in the presence of tartrate (Figure 10(b)). These results are significant not only because they explain the reduced deposition current density in the region of peak b, where tartrate works as an effective growth inhibitor, as already noted by other researchers [8–10], but also because they show that the tartrate works to reduce strain or cracking.

EDS showed no presence of carbon in the electrodeposit obtained in the presence of tartrate, at both deposition potentials, indicating that tartrate is not incorporated in the deposit.

Elucidation of the mechanism of growth inhibition and reduction of strain or cracking in the presence of tartrate will demand additional studies.

4. Conclusions

Both copper and tin were electrodeposited on to Pt substrates from a sulphuric acid solution, in the absence and presence of tartrate, at −0.310 and −0.640 V, as suggested by voltammetric curves and AAS analysis. The presence of tartrate as an additive in the plating bath did not increase the content of Cu or Sn in the deposits. Tartrate only modified the current density in

the more cathodic process. From the SEM results it can be inferred that tartrate favour a beneficial effect in the regions of first and second voltammetric peaks, leading to better quality deposits.

X-ray analysis of the deposits obtained at −0.310 V, in the presence or absence of tartrate, suggest the presence of a mixture of Cu and η-Cu_6Sn_5 alloy.

Acknowledgements

Financial support from Brazilian agencies FAPESP (Proc. No. 10145-4/98) and CNPq-RHAE (Proc. No. 610090/95) is gratefully acknowledged.

References

1. A. Brenner, ' Electrodeposition of Alloys. Principles and Practice', Vol. 1 (Academic Press, New York, 1963).
2. N.V. Parthasaradhy, 'Practical Electroplating Handbook' (Prentice-Hall, NJ, 1989).
3. F.A. Lowenheim, 'Modern Electroplating' (J. Wiley & Sons, New York, 1963).
4. K.L. Lee, C.K. Hu and K.N. Tu, *J. Appl. Phys.* **78** (1995) 4428.
5. K.N. Tu, *Mater. Chem. Phys.* **46** (1996) 217.
6. L. Missil, *Plat. Surf. Finish.* **10** (1978) 36.
7. S. Nisch and G. Rosesfeins, *Metal Finish.* **85** (1987) 188.
8. E. Michailova and A. Milchev, *J. Appl. Electrochem.* **21** (1991) 170.
9. G. Papanastasiou, D. Jannakoudakis, J. Amblard and M. Froment, *J. Appl. Electrochem.* **15** (1985) 71.
10. J. Amblard, M. Froment, C. Georgoulis and G. Papanastasiou, *Surf. Technol.* **6** (1978) 409.
11. S.S. Abd El Rehim, S.M. Abd El Wahaab, E.E. Fouad and H. H. Hassan, *J. Appl. Electrochem.* **24** (1994) 350.
12. P. Vanden Branden, A. Dumont and R. Winand, *J. Appl. Electrochem.* **24** (1994) 201.
13. L. Skibina, J. Stevanović and A.R. Despić, *J. Electroanal. Chem.* **310** (1991) 391.
14. S. Fletcher, *Electrochim. Acta* **28** (1983) 917.
15. B.J. Allen and L. Faulkner, 'Electrochemical Methods. Fundamentals and Applications' (J. Wiley & Sons, New York, 1980).
16. S. Kortly and L. Such, 'Handbook of Chemical Equilibria in Analytical Chemistry' (J. Wiley, New York, 1985).
17. F.A. Krogër, *J. Electrochem. Soc.* **125** (1978) 2028.
18. K.N. Tu, *Acta Metall.* **21** (1973) 347.
19. M. Hansen, 'Constitution of Binary Alloys', 2nd edn (McGraw-Hill, New York, 1958).
20. Joint Committee on Powder Diffraction Standards (JCPDS), *in* International Centre for Diffraction Data. Powder Diffraction File PDF-2. Database Sets 1–44. Pennsylvania, ICDD, 1994 (CDROM).